ON INTRINSIC THERMAL LIMITATIONS OF SUPER-CONDUCTING CAVITIES : KAPITZA RESISTANCE

J. Amrit*, C. Z. Antoine+, M. X. François* and H. Safa+

*LIMSI-CNRS, B.P. 133, Orsay, 91403, France

+CEA, DSM/DAPNIA/SEA, Saclay, 91191, France

ABSTRACT

Thermal behaviour of superconducting niobium cavities is investigated especially focusing on the Kapitza boundary resistance. First systematic measurements of the thermal boundary resistance are performed on samples with well characterised thermal conductivity (RRR values) and surface morphology (chemically etched or electropolished). The experimental data are used in a simple model, calculating the heat flux to the superfluid helium bath. These results show the relative importance of the Kapitza resistance with respect to the thermal conductivity. Also they indicate that best conditions are reached when using high RRR niobium with rough chemically etched outer surfaces.

INTRODUCTION

In the quest for higher accelerating gradients E_{acc} in particle accelerators much attention has been given to the influence of the inner surface state (chemically polished, electropolished, cleanliness with high pressure rinsing, ...) of the superconducting (s.c.) cavities. Indeed, it is now clear that the surface resistance R_s (mainly responsible for heat generation in the inner walls) and the surface state (mainly responsible for electron emission which absorbs available R.F. power and the now lesser important multipacting effect [1-2]) are some the dominant factors leading to thermal breakdown of these cavities. Among the other equally important limiting parameters we have the bulk thermal conductivity, κ of niobium and the Kapitza resistance, R_K at the outer surface of the cavity wall in contact with the He II refrigerant. Although the R_K has been evoked in different thermal studies and orders of magnitude used in calculations [3], there is still no systematic study of its importance on the thermal stability of s.c. cavities. In this paper we present first systematic measurements of the R_K for niobium samples having well characterised thermal conductivity and surface morphology. Further we attempt to quantify the relative

CP613, *Advances in Cryogenic Engineering: Proceedings of the Cryogenic Engineering Conference, Vol. 47,* edited by Susan Breon et al.

importance of the R_K (and therefore of surface morphology of the outer wall) by means of a thermal analysis of heat evacuation via a defect free cavity wall to He II.

The Kapitza Resistance

Heat exchange at the outer surface of the cavity wall in contact with superfluid helium is determined by the Kapitza resistance, defined as $R_K(cm^2K/W) = h_K^{-1} = \Delta T/\dot{q}$, where h_K is the Kapitza conductance, $\dot{q}$ the heat flux in W/cm^2 and $\Delta T = T_i - T_{bath}$, with T_i being the solid surface temperature in contact with He II and T_{bath} the helium temperature. The basic physical mechanism is that not all the phonons from the solid incident onto the interface couple into He II, and vice versa. In other words, the resistance arises from a non-unity phonon transmission coefficient τ across the interface. The expression for the Kapitza resistance can take the form : $R_K^{-1} = h_K = 1/4\, C_L v_L \langle \tau(\theta) \rangle$; where $C_L \propto T^3$ corresponds to the specific heat, v_L is the sound velocity in He II and $\langle \tau(\theta) \rangle$ is the average transmission coefficient from the liquid to the solid.

In the Khalatnikov model [4] the calculation of $\langle \tau(\theta) \rangle$ requires the conservation of the phonon frequency and the parallel component of the phonon wave vectors at the interface. For these conditions to be met the surface roughness must not exceed the phonon wavelengths which are of the order of 10-30 Å in helium at temperatures between 1 K and 2 K. In reality, the required conditions are not met and τ acquires a complex dependency on the sample surface state (roughness, chemical composition,...) as demonstrated by the dispersion in numerous experimental results [see for example ref.10 and references herein]. The exact physical origin of this dependency still remains to be discovered.

EXPERIMENTAL

Experimental cell and technique

An analysis of the experimental technique has been described in detail elsewhere [5]. We recall briefly that the Nb samples (flat disks of 5 cm in diameter and 2 mm in thickness) are mounted on either sides of a cylinder (1 cm in height), thus forming a cavity. This cavity is filled with He II and is placed in a temperature controlled (to within ~0.1mK) He II bath. For different steady state heat flux values, $\dot{q}$ dissipated in the cavity, the temperature increase in the latter is measured for a fixed bath temperature. From the resultant temperature difference ΔT and $\dot{q}$ values, the Kapitza resistance is determined using the relation:

$$R_K = \frac{\Delta T}{\dot{q}} - \frac{e}{2\kappa} \tag{1}$$

where e(cm) is the sample thickness. The thermal conductivity, κ in W/(cmK), of our samples were measured between 1.5 K and ~10 K [6].

Samples and their preparation

In order to reproduce as closely as possible the general procedure used in the preparation of s.c. cavities, we performed the following treatment. Additional mechanical and electro-polishing were applied in order to modify significantly the surface roughness.

The initial samples are disks of pure Nb (RRR=178 and of thickness 2 mm) supplied by Heraeus (G). These samples underwent one or more of the preparations described below:

1. Chemically etching

The Nb surface is ultrasonically degreased prior to any etching. The chemical etching is done in a mixture of HF(40%), HNO3 (69%), and H3PO4(85%) 1-1-2 in volume. It etches pure Nb at a rate of ~1-2 μm/min and allows to get rid of damaged surface layers and most of its surface impurities. In a standard procedure, at least ~30 μm are etched from the surface. This treatment produces a surface roughness of ~1-2 μm, depending on the origin of Nb.

2. Purification by annealing

Commercially available Nb can be characterised by a RRR of ~200-300. Moderate annealing (900°C-1300°C) of Nb in a vacuum and in presence of a getter material (titanium) allows to reduce considerably the main interstitial content (H, C, O) and to enhance the RRR value to ~600-700. This heat treatment leaves ~1 μm thick layer of titanium at the Nb surface which has to be removed by chemical etching. The resulting surface state is visually modified due to grain growth during annealing. However, the root mean square roughness, σ_{rms} is not affected significantly (see Table 1).

3. Mechanical and Electro-polishing

The samples are prepared on a rotating polishing machine, with SiC charged paper (800, 1000, and 1200 in size). This is followed by a short diamond paste (3 μm) polish on a tissue disk. Diamond paste tends to penetrate into the niobium and can also produce scratches on the surface. A finish is therefore carried-out using a felt with a colloidal suspension of silica in a slightly basic solution of oxygen peroxide. Mirror surfaces can be obtained ; nevertheless pure Nb is very soft and inclusions of the polishing material cannot be excluded. Therefore, in order to ensure removal of any foreign material at the surface a light electropolishing is performed afterwards in a HF-H_2SO_4 mixture.

We note that electropolishing is now widely adopted [7] as a necessary treatment of the inner surface of the cavity since it tends to give higher accelerating gradients, that is of the orders of 40 MV/m.

RESULTS AND DISCUSSIONS

Kapitza resistance measurements for different Nb samples

The characteristics of our samples including surface roughness, σ_{rms} determined with the aid of a stylus profiler (Dektak®), and the power laws (of the form αT^{-n}) fitting the R_K measurements are summarised in Table 1. Besides the RRR and R_K values, the distinctive feature of each sample is its surface morphology as shown in Figure 1. Indeed,

TABLE 1. Sample characteristics. The abbreviations used for the surface treatment stand for : CE chemically etched, EP electro-polished and A annealed. All values of R_K are in (cm^2K/W).

Sample # ; RRR	Surface Treatment	σ_{rms} (μm)	$R_K(cm^2K/W)$	R_K at T = 1.8K
#1 (●) ; 178	CE (~30μm)	1.8±0.4	$10.7xT^{-3.55}$	1.328
#2 (■) ; 178	EP	0.85±0.25	$21.3xT^{-4.11}$	1.902
#3 (◆) ; 647	A + CE (~30μm)	1.3±0.4	$16.1xT^{-3.93}$	1.598
#4 (▲) ; 647	A + CE + EP	0.2±0.1	$19.1xT^{-3.61}$	2.288

samples 1 and 2 have the same RRR values but radically different surface states. This is true for samples 3 and 4 as well. The chemically etched surfaces of samples 1 and 3 exhibit a grain structure revealed by preferential local etching. On the other hand, the electropolished samples 2 and 4 have a cupulated surface structure, as often observed on surfaces that have undergone heavy electropolishing. This effect is related to the local

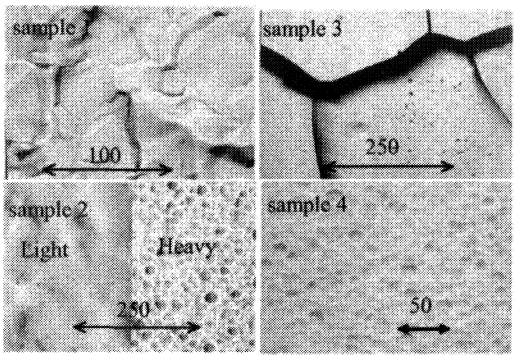

FIGURE 1. Surface micrography of the samples (see Table 1 for details). The scale length (in μm) is indicated.

profile and to the surface tension in the viscous layer of Nb during the dissolution process. The mean surface roughness of the electropolished samples is significantly reduced as compared to chemically etched samples.

Figure 2 shows R_K measurements of the samples between 1.5 K and $T_\lambda = 2.17$ K. The main source of error is due to the uncertainty in the thermal conductivity of the samples. The error bars vary from ~15% for the samples having RRR = 178 to ~5% for the annealed samples. The comparison of the R_K measurements for different σ_{rms} [8] (see Table 1) tends to corroborate the argument that the flatter the surface on a micro-metric scale the larger R_K. We emphasis the fact that this is not due to a change in the effective surface area, which is small, but to a modification of the transmission coefficient, that is, to a change in the physical mechanism governing heat exchange.

The annealing of sample 3 prior to a chemical etching leads to the apparition of distinct grain boundaries and larger grain sizes as compared to sample 1. Also, the thermal conductivity of sample 3 is improved by a factor of ~5 with respect to sample 1, whereas

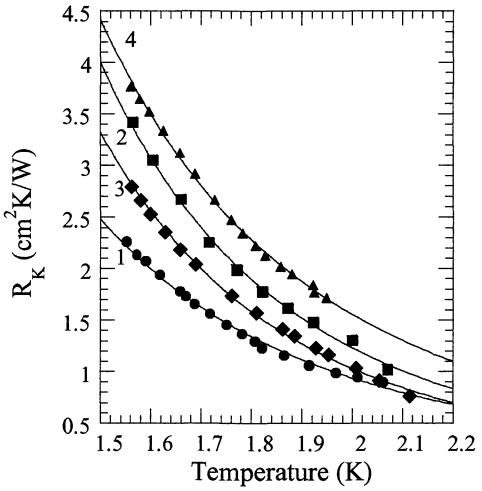

FIGURE 2. Measurements of the Kapitza resistance at the Nb-He II boundary for different samples as a function of temperature. Table 1 displays the characteristics of these samples.

the R_K measurements differ by ~15% only. Similar observations can be made for samples 2 and 4. It thus becomes apparent that the surface morphology on a micron scale plays a role more important than the bulk thermal conductivity in determining the magnitude of the R_K.

The Thermal-Magnetic Stability of S.C. Cavities

We now discuss the influence of R_K and κ on the accelerating field, E_{acc} based upon a simple heat transfer model. We shall consider that the heat flux $\dot{q}$ produced in W/m^2 by Joule heating at the inner surface wall is uniquely due to the rf surface resistance R_s, that is : $\dot{q} = (1/2\mu_o^2)R_s B^2$, where μ_o is the magnetic permeability, B, expressed in tesla, is the magnetic flux density on the inner surface of the cavity and R_s is in ohms. We recall that $E_{acc} \propto B$. Although this is somewhat of an "ideal" situation, it helps to highlight the relative importance of κ and R_K on the thermal stability and on the maximum achievable magnetic fields. Also, in the case of defects, the basic mechanism is essentially the same with higher heat fluxes and smaller magnetic fields.

Figure 3 shows an element of the cavity wall in contact with He II and its electrical analogue of the heat flow path to the He II bath. The procedure adopted for the calculations is as follows. For a given T_{bath} we calculate $\dot{q}$ and T_i as a function of T_s using :

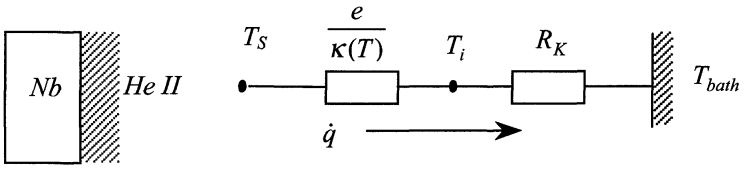

FIGURE 3. Electrical analogy of heat transfer from the solid to He II.

$$\Delta T = T_s - T_{bath} = \left(\frac{e}{\kappa_m} + R_K \right) \dot{q} \tag{2}$$

and

$$(T_i - T_{bath}) = R_K \dot{q} \tag{3}$$

with

$$\kappa_m = \frac{1}{T_s - T_i} \int_{T_i}^{Ts} \kappa(T) dT \tag{4}$$

In the first step of the iteration T_i is set to T_{bath}. The heat flux $\dot{q}$ calculated from (2) is used to determine the new T_i from (3). The latter is used to recalculate κ_m which in turn is substituted in (2) and the process is repeated. We consider that optimal values of $\dot{q}$ and T_i are reached when the temperature difference between successive iterations converges to within 10^{-4} K. We add that the thermal conductivity of the samples having different RRR values were measured over a wide temperature range.

Strictly speaking, T_i is the temperature of the solid surface in contact with the He II. We also note that all calculations were done for T_{bath} = 1.8 K and for the cavity wall thickness set to the generally used value of 2.8 mm. For the surface resistance, we used the expression $R_s = R_{BCS} + R_{res}$, where $R_{BCS} = (A/T)\exp(-1.76T/T_c)$ with $A = 1219.4\,\text{n}\Omega/\text{K}$ [9], the Nb transition temperature, $T_c = 9.2$ K and the residual resistance, $R_{res} = 4\,\text{n}\Omega$.

Figure 4a shows that each solid surface reaches T_λ at different heat flux values depending on the Kapitza resistance only. However the actual heat flux evacuated from the solid to He II depends on the combined effects of κ and R_K as clearly put to evidence in Figure 4b. The large heat flux regime is defined generally for $\dot{q} \geq 1000$ W/m^2. In this case the solid surface can attain temperatures above T_λ whereas T_{bath} still remains below T_λ. Also, the critical heat flux for which phase changes occur in He II depends mainly on the bulk properties of He II and on the heating duration [10].

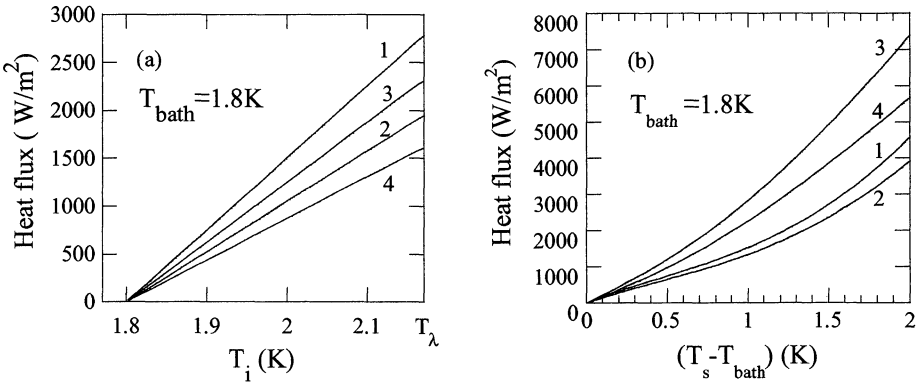

FIGURE 4a. Heat flux in (W/m^2) as a function of the outer solid surface temperature, T_i.

FIGURE 4b. Heat flux dependency on the thermal conductivity and the Kapitza resistance for different samples.

The calculated magnetic field density as a function of the inner wall temperature, T_s is shown in Figure 5 by the continuous solid thick lines and the dotted lines, which represent a nonphysical solution. Also indicated in the figure, by the continuous curves, is the interface temperature as a function of T_s for each sample. The dashed line corresponds to the theoretical limit of the critical magnetic field, $B_c = B_{c2}[1-(T/T_c)^2]$, with the superheating field, B_{c2} = 240 mT. The calculated magnetic fields exceed the B_c field. This is due to the somewhat "ideal" values of R_s which were used in the calculations. It is important to note that the relative variations in the calculated magnetic fields due to the effects of R_K and κ_m remain unchanged for more realistic values of R_s in the case of defect-free cavities.

The effect of an increased thermal conductivity on the magnetic field is clearly apparent from comparing curves of samples of RRR = 647 and RRR = 178. At the maximum attainable magnetic fields, sample sets 1 and 3 and sample sets 2 and 4 have the similar R_K values (see Table 1). This is so because the maximum magnetic fields occur at different interface temperatures depending on the surface nature of each sample as shown in Figure 5. Consequently, the relative increase of ~ 20% in the maximum magnetic field of sample 3 (RRR = 647) arises solely from its high thermal conductivity with respect to that of sample 1 (RRR = 178). This effect is also observed for samples 2 and 4. We note that experimentally obtained maximum accelerating fields also show an increase with the RRR values (see Figure 23 in [9]).

Sample 3 and 4, which have both a RRR of 647 , [and samples 1 and 2, which have a RRR of 178] have the same bulk thermal conductivity but different R_K behaviour with temperature due to their surface morphology (see Figure 1 and Table 1). The relative gain

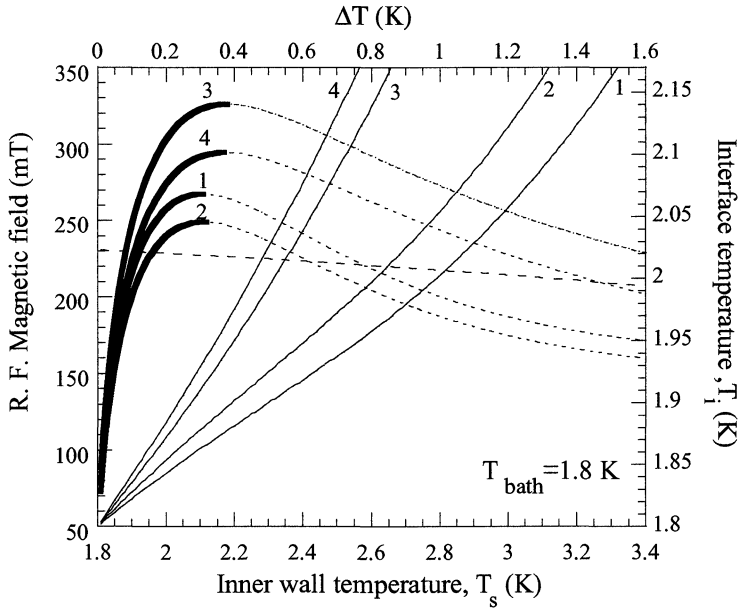

FIGURE 5. Calculated magnetic field density in mT (thick continuous and dotted lines) as function of T_s for samples of niobium. The second x-axis corresponds to the temperature difference between T_s and T_{bath}. Also indicated (by the continuous lines) are the interface temperatures as a function of T_s for each sample. The dashed line represents the maximum theoretical magnetic field. Same sample numbers used as in Table 1.

in the maximum magnetic field of sample 3, with respect to sample 4, is $\sim 11\%$; whereas sample 1 has a relative gain of $\sim 7\%$ compared to sample 2. These results firstly highlight, for a given RRR value, the importance of having a low R_K in achieving a maximum accelerating field. Secondly they tend to show that the influence of R_K increases especially when the thermal conductivity (RRR) is improved. Thirdly, the combined effects of an increased thermal conductivity and a low Kapitza resistance (as in the case of chemically polished samples surfaces) can lead to a relative gain on the maximum attainable field by magnitudes as large as 30%, as demonstrated by samples 2 and 3.

CONCLUSION

A systematic study of the effects of different surface morphology, resulting from purification by annealing and/or chemical polishing or electropolishing, on the Kapitza resistance at the sample-He II boundary has been conducted. The results clearly show that the Kapitza resistance is smaller for chemically etched surfaces as compared to the electropolished surfaces for polycrystalline niobium. These samples were characterised on a micron scale and they show significant differences in roughness and in their aspect. Thus it becomes apparent from this study that surface roughness at a micron scale has an effect on the heat exchange mechanism at the boundary. The effects of these surface treatments are unknown on scale lengths smaller than a 0.1 μm since large scale roughness tend to mask small scale roughness. We recall however, that the phonons in the superfluid He have wavelengths of the order of ~1-2 nm at $T \geq 1K$. And it would be interesting to know the influence of roughness at a nano-metric scale on the heat transfer at the boundary in order to get a better understanding of the physical mechanism leading to the Kapitza resistance. This may possibly help to further reduce the R_K.

We have also quantified the relative importance of the Kapitza resistance with respect to the bulk thermal conductivity, on the induced heat flux and the magnetic field. The results clearly show the need for high thermal conductivity niobium. In this case the Kapitza resistance becomes equally an important, if not, the dominant limiting factor leading to a thermal–magnetic breakdown.

REFERENCES

1. Padamsee, H., Knobloch, J. and Hays, T., *RF Superconductivity for Accelerators*, John Wiley, New York, 1998, ch.11.
2. Krafft, K.R., "Thermal transport and thermal-magnetic breakdown in superconducting cavities made of high thermal conductivity niobium", (Ph.D. thesis), Cornell University, 1983.
3. Isawaga, S. and Isawaga, K., *Cryogenics*, **20**, pp. 677 (1980).
4. Khalatnikov I. M., *Introduction to the Theory of Superfluidity,* Benjamin, New York, 1965, ch. 23.
5. Amrit, J. and François, M.X., *J. Low Temp. Phys.* **119**, (1/2), pp. 27 (2000).
6. Measurements were done at the CEA/SEA.
7. Safa, H., "Progress and trends in SCRF cavities for future accelerators", in *Proceedings of EPAC*, Vienna, Austria, 2000.
8. The variation range of the roughness values in Table 1 is dominated by the discrepancies of the surface state of a sample and not by the measurement uncertainty.
9. Aune, B., *et al*, "The Superconducting TESLA Cavities", in *Phys. Rev.STAccel.Beams* **3**, (2000).
10. Pfotenhauer J. M. and Donnelly R. J., "Heat transfer in liquid helium", in *Advances in Heat Transfer*, **17**, pp. 65 (1985).